Reactions of the Co-ordinatively Unsaturated Cluster $[Os_3(\mu\text{-}H)(CO)_8\{Ph_2PCH_2P(Ph)C_6H_4\}]$ with Alkynes RC≡CR (R = Ph, C_6H_4Me, Me or CF_3); Crystal Structures of $[Os_3(CO)_8\{\mu_3\text{-}\eta^2(\|)\text{-}RC_2R\}(Ph_2PCH_2PPh_2)]$ (R = Me or CF_3) and Electrochemical Behaviour of Triosmium–Alkyne Clusters†

Michael P. Brown,[a] P. Ann Dolby,[a] Marjorie M. Harding,[a] A. Jane Mathews,[a] Anthony K. Smith,*[,a] Domenico Osella,*[,b] Mauro Arbrun,[b] Roberto Gobetto,[b] Paul R. Raithby[c] and Piero Zanello[d]

[a] *Department of Chemistry, University of Liverpool, P.O. Box 147, Liverpool L69 3BX, UK*

[b] *Dipartimento di Chimica Inorganica, Chimica Fisica e Chimica dei Materiali, Università di Torino, Via P. Giuria 7, 10125 Torino, Italy*

[c] *University Chemical Laboratory, Lensfield Road, Cambridge CB2 1EW, UK*

[d] *Dipartimento di Chimica, Università di Siena, Pian dei Mantellini 44, 53100 Siena, Italy*

Treatment of the unsaturated triosmium cluster $[Os_3(\mu\text{-}H)(CO)_8\{\mu\text{-}Ph_2PCH_2P(Ph)C_6H_4\}]$ **1** with diphenylacetylene leads to the formation of $[Os_3(CO)_7(PhC_2Ph)(Ph_2PCH_2PPh_2)]$ **2a** in which the alkyne is bonded in a $\mu_3\text{-}\eta^2$ (⊥) mode. Addition of CO to **2a** gives $[Os_3(CO)_7(\mu\text{-}CO)(RC_2R)(Ph_2PCH_2PPh_2)]$ **3a** (R = Ph) in which the alkyne is bonded in a $\mu_3\text{-}\eta^2(\|)$ mode. Two-electron electrochemical reduction of **2a** also causes this change in co-ordination mode of the alkyne ligand. Protonation of the electrochemically produced dianion $[Os_3(CO)_7\{\mu_3\text{-}\eta^2(\|)PhC_2Ph\}(Ph_2PCH_2PPh_2)]^{2-}$ gives $[Os_3(\mu\text{-}H)_2(CO)_7\{\mu_3\text{-}\eta^2(\|)\text{-}PhC_2Ph\}(Ph_2PCH_2PPh_2)]$ **4**. The same product **4** has also been obtained by direct hydrogenation of **2a**. A similar chemical and electrochemical behaviour is observed for the ditolylacetylene derivative $[Os_3(CO)_7(p\text{-}MeC_6H_4C_2C_6H_4Me\text{-}p)(Ph_2PCH_2PPh_2)]$ **2b**, where the two *p*-methyl substituents are diagnostic in ^1H NMR spectroscopy. With the alkynes RC≡CR (R = Me or CF_3), analogous complexes to **2** are not observed, instead complexes $[Os_3(CO)_8\{\mu_3\text{-}\eta^2(\|)\text{-}RR\}(Ph_2PCH_2PPh_2)]$ **3c** (R = Me) and **3d** (R = CF_3) are obtained. Single-crystal X-ray structure determinations of **3c** and **3d** have been performed.

The co-ordination mode of an alkyne to triangular metal clusters has been shown to be dependent on both the metal and the substituents on the alkyne.[1] Thus, with terminal alkynes, HC≡CR, reaction of metal clusters often leads to hydrogen transfer to the metal, whereas with alkynes of the type RC≡CR either a $\mu_3\text{-}\eta^2(\perp)$ mode, or more commonly, a $\mu_3\text{-}\eta^2(\|)$ mode of co-ordination is observed (Fig. 1).[1] The perpendicular co-ordination mode is seen in $[Fe_3(CO)_9(PhC_2Ph)]$[2] and $[Fe_2Ru(CO)_9(RC_2R)]$ (R = Et or Ph),[3] and is probably present in the highly reactive species $[Os_3(CO)_9(PhC_2Ph)]$.[4] The parallel co-ordination mode is observed in $[M_3(CO)_{10}(RC_2R)]$ (R = Me, Et, Ph, CO_2H or CO_2Me),[5–10] $[M_3H_2(CO)_9(C_8H_8)]$[11] (M = Ru or Os), and several heterometallic cluster alkyne complexes.[12] It thus appears that the perpendicular co-ordination mode is observed in 46-electron clusters, and is stabilised by back donation from the metal atoms to the alkyne.[13–15] When the back-donation ability is decreased the alkyne adopts a parallel co-ordination mode and the cluster adopts a 48-electron configuration. Thus, $[Fe_3(CO)_9\{\mu_3\text{-}\eta^2(\perp)\text{-}RC_2R\}]$ (R = Et or Ph) is stable whereas the decreased back-donation ability of ruthenium and osmium compared to iron leads to the formation of $[M_3(CO)_{10}\{\mu_3\text{-}\eta^2(\|)\text{-}RC_2R\}]$ (M = Ru or Os). However, by the electrochemical addition of two electrons to the 46-electron triiron cluster, it has been shown that the co-ordination mode of the alkyne is changed from perpendicular to parallel in a chemically reversible manner.[16] This relationship between cluster electron count and alkyne bonding mode is thus firmly established. However, the alkynetrirhodium cluster $[Rh_3(C_5H_5)(acac)(CO)(CF_3C_2CF_3)]$ (acac = acetylacetonate) has recently been reported to violate this pattern.[17]

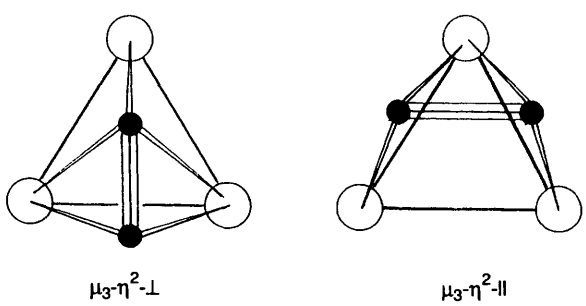

Fig. 1 Sketch of the two bonding modes between an internal alkyne and a trimetallic cluster. The ⊥ mode has been determined for **2a** and suggested for **2b**. The ‖ mode has been determined for **3c** and **3d** and suggested for **3a**, **3b** and **4**

In a preliminary communication[18] we reported the formation of $[Os_3(CO)_7\{\mu_3\text{-}\eta^2(\perp)\text{-}PhC_2Ph\}(Ph_2PCH_2PPh_2)]$ in which the co-ordination of phosphine ligands to osmium was suggested to increase the back-donating ability of the metal atoms and thus allow the perpendicular co-ordination mode of the alkyne to be stabilised. Recently, the analogous ruthenium complex $[Ru_3(CO)_7\{\mu_3\text{-}\eta^2(\perp)\text{-}PhC_2Ph\}(Ph_2PCH_2PPh_2)]$ has been reported.[19] This complex undergoes a reversible

† *Supplementary data available:* see Instructions for Authors, *J. Chem. Soc., Dalton Trans.*, 1993, Issue 1, pp. xxiii–xxviii.

Table 1 Spectroscopic data

Complex	NMR (δ) $^{31}P-\{^1H\}$[a]	^1H[b]	IR (cm^{-1}) ν(CO)[c]
2a	3.77 (s)	7.4–6.6 (m, 30, Ph), 3.74–2.84 (m, 2, CH_2)[d]	2052m, 1980s, 1960 (sh), 1920w
2b	4.00 (s)	7.5–6.6(m,28,Ph),3.78–2.86(m,2,CH_2),[d]2.20(s,3,CH_3),2.15(s,3,CH_3)	2058m, 1987s, 1973 (sh), 1924w
3a	−4.95 (s)	7.9–7.3 (m, 30, Ph), 5.00–3.63 (m, 2 CH_2)[d]	2055m, 2000vs, 1995vs, 1980s, 1965m, 1800w (br)
3b	−2.74 (s)	7.4–6.8 (m, 28, Ph), 4.60–3.22 (m, 2, CH_2),[d] 2.22 (s, 6, CH_3)	2056m, 1988vs, 1967m, 1958 (sh), 1790w (br)
3c	−2.77 (s)	7.6–7.0 (m, 20, Ph), 5.10–4.30 (m, 2, CH_2),[d] 2.22 (s, 6, CH_3)	2050m, 2010vs, 1990vs, 1955m, 1970w (br)
3d	−1.51 (s)	7.3–6.7 (m, 20, Ph), 5.30–4.27 (m, 2, CH_2),[d] −54.1 (s, CF_3)[e]	2073m, 2023s, 1988m, 1975 (sh), 1815w (br)
4	−2.30 (s)	7.8–6.3 (m, 20, Ph), 4.10–2.90 (m, 2, CH_2),[d] −15.15 (t, 1, J_{PH} 12.5), −19.34 (d, 1, J_{PH} 32)	2092w, 2058vs, 2024m, 1995s, 1978s, 1938w

[a] Recorded in $CDCl_3$ solution at 162.1 MHz, referred to 85% H_3PO_4 (δ = 0). [b] Recorded in $CDCl_3$ at 400 MHz, referred to $SiMe_4$ (δ = 0). [c] Recorded in CH_2Cl_2. [d] The CH_2 group of the $Ph_2PCH_2PPh_2$ ligands appears as two multiplets readily interpreted as an ABX_2 (X = ^{31}P) system. This is in agreement with the axial co-ordination mode of the $Ph_2PCH_2PPh_2$ ligand as found in the solid-state structure of **2a**, **3c** and **3d**. [e] ^{19}F resonance.

reaction with CO in which the co-ordination mode of the alkyne changes from ⊥ to ∥. We now provide full details of the triosmium alkyne work and the syntheses of other alkyne derivatives (RC≡CR; R = C_6H_4Me, Me or CF_3) of the diphosphine-substituted triosmium cluster, together with an electrochemical study of all these compounds.

Results and Discussion

Syntheses and Characterisation of Alkynetriosmium Clusters.—Treatment of the unsaturated cluster $[Os_3H(CO)_8\{Ph_2PCH_2P(Ph)C_6H_4\}]$ **1** with an excess of diphenylacetylene gives rise to a red solution from which, after purification by TLC, a red crystalline solid, $[Os_3(CO)_7(PhC_2Ph)(Ph_2PCH_2PPh_2)]$ **2a** is isolated in good yield. The crystal structure of this complex, reported in a preliminary communication,[18] shows that the alkyne is co-ordinated in a μ_3-η^2(⊥) mode. Complex **2a** is a 46-electron triangular cluster and thus is expected to undergo two-electron addition reactions to achieve a saturated 48-electron structure. It is also to be expected that in this corresponding 48-electron cluster the alkyne ligand would change to a μ_3-η^2(∥) co-ordination mode.[16] In agreement with this, we have found that complex **2a** reacts with CO to give $[Os_3(CO)_8(PhC_2Ph)(Ph_2PCH_2PPh_2)]$ **3a**, and undergoes a single-step two-electron reduction at a mercury or platinum electrode to give $[Os_3(CO)_7(PhC_2Ph)(Ph_2PCH_2PPh_2)]^{2-}$ (see below) in which the diphenylacetylene ligand adopts the μ_3-η^2(∥) co-ordination mode. Thus, bubbling CO through a toluene solution of **2a** at room temperature for 15 min causes a change in colour from red to orange, due to the formation of **3a**. This complex has been characterised by NMR and IR spectroscopy (Table 1), and mass spectrometry. The data show that the phosphorus atoms are equivalent and that the structure contains a bridging CO ligand (ν_{CO} 1800 cm^{-1}). The data are consistent with a μ_3-η^2(∥) co-ordination mode of the alkyne, analogous to that found for $[Os_3(CO)_8(RC_2R)(Ph_2PCH_2PPh_2)]$ (R = CF_3 or Me) (see below). More diagnostic of the alkyne rearrangement are the ^{13}C NMR spectroscopic data, obtained using enriched samples. The room-temperature $CDCl_3$, spectrum of **2a** exhibits, in the carbonyl region, three resonances at δ 184.3, 183.3 and 176.0 in the ratio of 2:2:3 respectively [Fig. 2(*a*)]. The broadening of the two downfield resonances (due to unresolved geminal $^{31}P-^{13}C$ coupling) enables them to be assigned to the carbonyls attached to the $Os(CO)_2P$ moieties, and the remaining resonance at δ 176.0 is thus assigned to the carbonyls of the $Os(CO)_3$ unit which will be undergoing rapid localised exchange at room temperature. Treatment of the sample with ^{13}CO in a sealed NMR tube produces a change in the spectrum concomitant with the

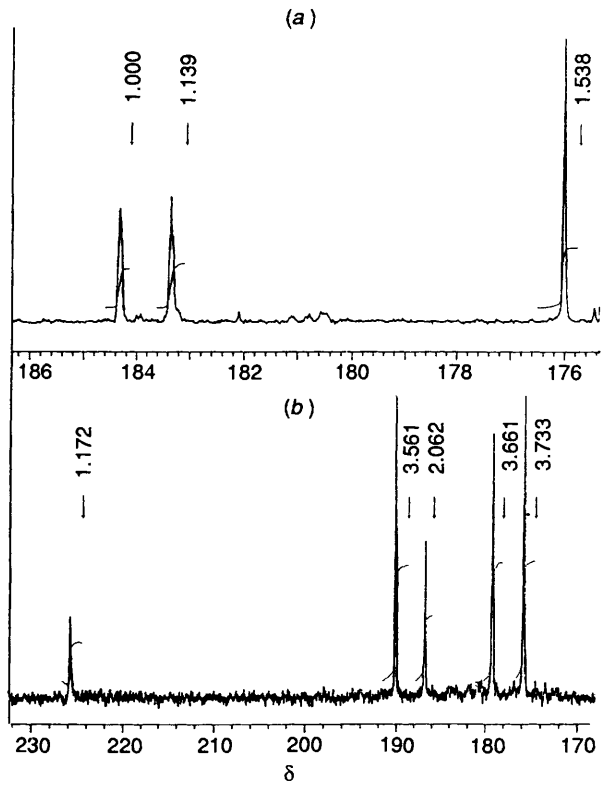

Fig. 2 Carbon-13 NMR spectra in $CDCl_3$ solution of ^{13}CO enriched samples of (*a*) compound **2a** at room temperature; (*b*) **3a** at −60 °C

2a ⟶ **3a** transformation. Two very broad signals are observed at room temperature, indicating a rapid dynamic process occurring in **3a**. The low-temperature-limiting spectrum is reached at −60 °C where five resonances are observed at δ 225.8, 190.1, 186.8, 179.2 and 175.8 of relative intensity 1:2:1:2:2 [Fig. 2(*b*)]. The lowest-field resonance is assigned to the bridging CO and the highest-field resonances, at δ 179.2 and 175.8 to the $Os(CO)_2P$ unit (unresolved $^{31}P-^{13}C$ couplings are observed in the expanded spectrum). The resonances at δ 190.1 and 186.8 (in the ratio of 2:1) are due to the equatorial and axial carbonyls of the $Os(CO)_3$ moiety which are rigid at −60 °C. Thus the ^{13}C NMR data confirm the addition of a CO group in a bridging position and the change in geometry of the cluster. Unfortunately no acetylenic carbon resonances (at natural abundance) could be observed due to the poor solubility of **2a**

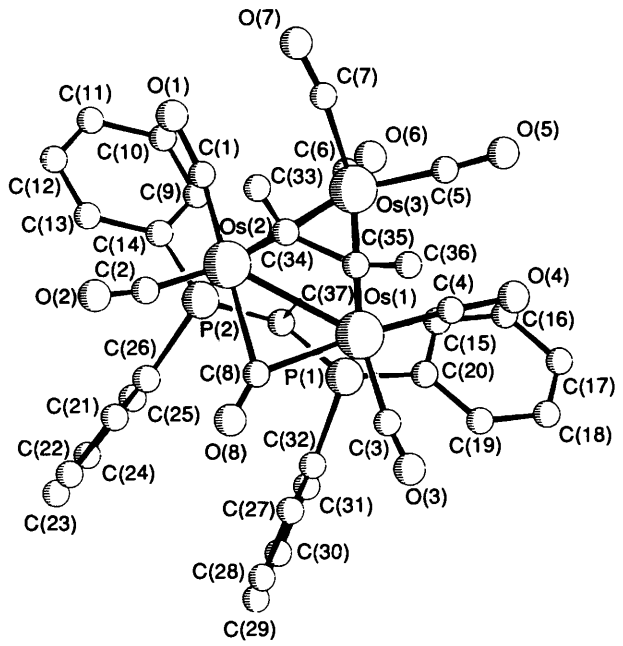

Fig. 3 The molecular structure of $[Os_3(CO)_8(MeC_2Me)(Ph_2PCH_2PPh_2)]$ **3c**, with hydrogen atoms omitted

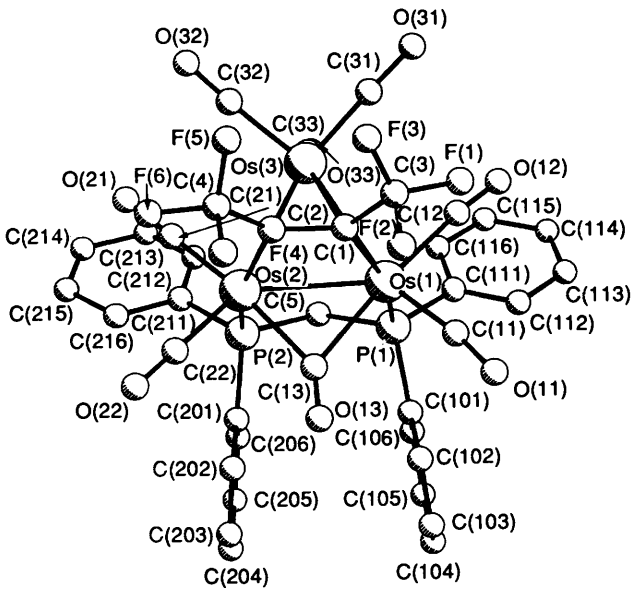

Fig. 4 The molecular structure of $[Os_3(CO)_8(CF_3C_2CF_3)(Ph_2PCH_2PPh_2]$ **3d**, with hydrogen atoms omitted

and **3a**. The phenyl-substituent resonances in the ^{13}C and ^1H NMR spectra are not diagnostic due to the overlap which occurs between these resonances and those of the phenyl groups of the $Ph_2PCH_2PPh_2$ ligand. In order to obtain further evidence of the $\perp \longrightarrow \parallel$ arrangement of the alkyne ligand and to employ this probe in the exhaustive electrolysis (see below) we synthesised the ditolylacetylene derivative $[Os_3(CO)_7(p\text{-}MeC_6H_4C_2C_6H_4Me\text{-}p)(Ph_2PCH_2PPh_2)]$ **2b** using an identical procedure to that for **2a**. The IR and NMR spectroscopic data for **2b** are similar to those of **2a** (Table 1) indicating a similar structure. Interestingly, the ^1H NMR spectrum of **2b** shows, in addition to the multiplets of Ph and the ABX_2 system of the CH_2 group, two singlets at δ 2.20 and 2.15 due to inequivalent methyl groups of the tolyl units, indicating an asymmetrical (*i.e.* perpendicular) co-ordination mode of the $p\text{-}MeC_6H_4C{\equiv}CC_6H_4Me\text{-}p$ alkyne. Treatment of **2b** with CO leads to the formation of $[Os_3(CO)_8(p\text{-}MeC_6H_4C_2C_6H_4Me\text{-}p)(Ph_2PCH_2PPh_2)]$ **3b**, the spectral patterns of which are similar to those of **3a** (Table 1). In the ^1H NMR spectrum of **3b** a single resonance at δ 2.22 for the methyl groups of the ditolylacetylene is observed, indicating a more symmetric (*i.e.* parallel) co-ordination mode of the alkyne.

The reaction of compound **1** with RC≡CR (R = Me or CF_3) in toluene solution at 80 °C gives the symmetrical clusters $[Os_3(CO)_8(RC_2R)(Ph_2PCH_2PPh_2)]$ (R = Me **3c** or CF_3 **3d**) in good yield as the major product (for spectroscopic data see Table 1). No evidence for the formation of products analogous to the $\mu_3\text{-}\eta^2(\perp)$-PhC≡CPh complex **2a** was found. The crystal structures of **3c** and **3d** were determined. The structures are shown in Figs. 3 and 4 respectively, and lists of bond lengths and angles are given in Tables 2 and 3 and atom parameters in

Table 2 Bond lengths (Å) and angles (°) for $[Os_3(CO)_8(MeC_2Me)(Ph_2PCH_2PPh_2)]$ **3c**

Os(1)–Os(2)	2.810(1)	Os(1)–C(3)	1.91(3)
Os(1)–Os(3)	2.758(1)	Os(1)–C(4)	1.88(4)
Os(2)–Os(3)	2.766(2)	Os(2)–C(1)	1.88(3)
Os(1)–P(1)	2.404(6)	Os(2)–C(2)	1.94(2)
Os(2)–P(2)	2.381(7)	Os(3)–C(5)	1.89(5)
Os(1)–C(35)	2.10(3)	Os(3)–C(6)	1.93(3)
Os(3)–C(35)	2.28(2)	Os(3)–C(7)	1.92(2)
Os(2)–C(34)	2.08(2)	Os(1)–C(8)	2.14(4)
Os(3)–C(34)	2.25(2)	Os(2)–C(8)	2.18(3)
C(34)–C(35)	1.41(4)	P(1)–C(20)	1.83(2)
C(33)–C(34)	1.60(3)	P(1)–C(32)	1.81(2)
C(35)–C(36)	1.56(4)	P(2)–C(14)	1.81(2)
P(1)–C(37)	1.83(3)	P(2)–C(26)	1.83(3)
P(2)–C(37)	1.82(3)		
Os(2)–Os(1)–Os(3)	59.6(1)	Os(2)–C(34)–Os(3)	79.4(7)
Os(1)–Os(2)–Os(3)	59.3(1)	Os(1)–C(35)–Os(3)	77.9(9)
Os(1)–Os(3)–Os(2)	61.2(1)	C(1)–Os(2)–C(2)	93.4(14)
Os(2)–Os(1)–P(1)	92.9(2)	C(3)–Os(1)–C(4)	91.2(10)
Os(3)–Os(1)–P(1)	108.8(1)	C(5)–Os(3)–C(6)	93.4(11)
Os(1)–Os(2)–P(2)	93.0(2)	C(5)–Os(3)–C(7)	93.5(14)
Os(3)–Os(2)–P(2)	109.4(2)	C(6)–Os(3)–C(7)	94.3(12)
Os(1)–Os(2)–C(34)	70.8(5)	Os(2)–C(8)–Os(1)	81.0(10)
Os(2)–Os(1)–C(35)	43.3(5)	P(1)–C(37)–P(2)	114(2)
Os(3)–Os(2)–C(35)	47.6(5)	C(33)–C(34)–C(35)	124(2)
Os(3)–Os(2)–C(34)	53.0(5)	C(34)–C(35)–C(36)	123(2)

Table 3 Bond lengths (Å) and angles (°) for $[Os_3(CO)_8(CF_3C_2CF_3)(Ph_2PCH_2PPh_2)]$ **3d**

Os(1)–Os(2)	2.818(2)	Os(1)–C(11)	1.84(3)
Os(1)–Os(3)	2.785(2)	Os(1)–C(12)	1.99(3)
Os(2)–Os(3)	2.790(2)	Os(2)–C(21)	1.79(4)
Os(1)–P(1)	2.377(7)	Os(2)–C(22)	1.90(3)
Os(2)–P(2)	2.389(7)	Os(3)–C(31)	1.84(5)
Os(1)–C(1)	2.09(3)	Os(3)–C(32)	1.90(4)
Os(3)–C(1)	2.24(3)	Os(3)–C(33)	1.87(3)
Os(2)–C(2)	2.09(3)	Os(1)–C(13)	2.25(2)
Os(3)–C(2)	2.18(3)	Os(2)–C(13)	2.17(2)
C(1)–C(2)	1.36(4)	P(1)–C(101)	1.83(2)
C(1)–C(3)	1.58(5)	P(1)–C(111)	1.83(2)
C(2)–C(4)	1.57(4)	P(2)–C(201)	1.83(2)
P(1)–C(5)	1.84(3)	P(2)–C(211)	1.83(2)
P(2)–C(5)	1.84(3)		
Os(2)–Os(1)–Os(3)	59.7(1)	Os(2)–C(2)–Os(3)	81.8(9)
Os(1)–Os(2)–Os(3)	59.5(1)	Os(1)–C(1)–Os(3)	80.1(9)
Os(1)–Os(3)–Os(2)	60.7(1)	C(21)–Os(2)–C(22)	89.4(14)
Os(2)–Os(1)–P(1)	93.0(2)	C(11)–Os(1)–C(12)	88.0(13)
Os(3)–Os(1)–P(1)	111.3(2)	C(31)–Os(3)–C(32)	91.6(18)
Os(1)–Os(2)–P(2)	93.1(2)	C(31)–Os(3)–C(33)	90.6(18)
Os(3)–Os(2)–P(2)	110.2(2)	C(32)–Os(3)–C(33)	94.0(14)
Os(1)–Os(2)–C(2)	69.3(7)	Os(1)–C(13)–Os(2)	79.1(8)
Os(2)–Os(1)–C(1)	69.8(7)	P(1)–C(5)–P(2)	113.4(13)
Os(3)–Os(2)–C(2)	50.5(7)	C(3)–C(1)–C(2)	127(3)
Os(3)–Os(1)–C(1)	52.4(7)	C(1)–C(2)–C(4)	125(2)

Table 4 Atomic coordinates for $[Os_3(CO)_8(MeC_2Me)(Ph_2PCH_2PPh_2)]$ **3c**

Atom	*x*	*y*	*z*	Atom	*x*	*y*	*z*
Os(1)	0.781 37(10)	0.882 08(7)	0.119 70(6)	C(13)	0.402 0(18)	0.845 7(11)	0.348 6(12)
Os(2)	0.652 12(11)	0.791 14(7)	0.217 08(6)	C(14)	0.471 1(18)	0.905 3(11)	0.325 7(12)
Os(3)	0.846 70(12)	0.846 18(7)	0.267 35(6)	C(15)	0.740 9(19)	1.131 1(13)	0.200 6(10)
P(1)	0.663 6(6)	0.993 2(4)	0.125 0(4)	C(16)	0.804 9(19)	1.198 0(13)	0.202 8(10)
P(2)	0.523 1(6)	0.892 7(4)	0.229 4(4)	C(17)	0.859 4(19)	1.221 9(13)	0.136 8(10)
C(1)	0.639 6(30)	0.772 0(19)	0.323 4(22)	C(18)	0.849 8(19)	1.179 0(13)	0.068 6(10)
C(2)	0.557 7(23)	0.705 3(13)	0.189 6(18)	C(19)	0.785 8(19)	1.112 1(13)	0.066 4(10)
C(3)	0.810 3(19)	0.878 1(19)	0.011 6(16)	C(20)	0.731 4(19)	1.088 1(13)	0.132 4(10)
C(4)	0.897 3(27)	0.950 1(22)	0.136 0(16)	C(21)	0.382 9(21)	0.834 5(14)	0.116 6(15)
C(5)	0.990 5(39)	0.877 1(24)	0.264 8(21)	C(22)	0.291 1(21)	0.837 3(14)	0.071 7(15)
C(6)	0.802 9(17)	0.938 9(17)	0.323 1(11)	C(23)	0.219 3(21)	0.899 1(14)	0.080 8(15)
C(7)	0.864 8(25)	0.783 4(25)	0.358 7(14)	C(24)	0.239 5(21)	0.958 2(14)	0.134 7(15)
C(8)	0.655 7(34)	0.802 3(19)	0.091 7(17)	C(25)	0.331 3(21)	0.955 4(14)	0.179 5(15)
O(1)	0.631 0(26)	0.754 4(21)	0.388 5(16)	C(26)	0.403 0(21)	0.893 6(14)	0.170 4(15)
O(2)	0.524 1(26)	0.645 5(9)	0.185 1(15)	C(27)	0.551 3(19)	0.960 4(11)	−0.009 8(12)
O(3)	0.825 9(37)	0.868 7(15)	−0.050 8(13)	C(28)	0.472 5(19)	0.974 6(11)	−0.064 5(12)
O(4)	0.973 1(20)	0.993 0(16)	0.139 2(11)	C(29)	0.409 3(19)	1.041 8(11)	−0.058 7(12)
O(5)	1.081 3(22)	0.891 5(25)	0.262 3(19)	C(30)	0.425 2(19)	1.094 7(11)	0.001 7(12)
O(6)	0.775 8(27)	0.994 4(16)	0.353 5(17)	C(31)	0.504 1(19)	1.080 5(11)	0.056 3(12)
O(7)	0.875 3(23)	0.749 9(24)	0.411 4(16)	C(32)	0.567 2(19)	1.013 3(11)	0.050 6(12)
O(8)	0.613 5(22)	0.773 8(18)	0.040 7(13)	C(33)	0.826 9(18)	0.649 3(17)	0.233 4(21)
C(9)	0.499 7(18)	0.964 3(11)	0.377 6(12)	C(34)	0.798 3(19)	0.736 2(11)	0.204 5(13)
C(10)	0.459 3(18)	0.963 6(11)	0.452 5(12)	C(35)	0.862 6(29)	0.779 9(19)	0.153 6(11)
C(11)	0.390 3(18)	0.903 9(11)	0.475 4(12)	C(36)	0.973 0(22)	0.751 4(22)	0.125 1(15)
C(12)	0.361 6(18)	0.845 0(11)	0.423 5(12)	C(37)	0.578 1(27)	0.989 8(29)	0.210 4(15)

Table 5 Atomic coordinates for $[Os_3(CO)_8(CF_3C_2CF_3)(Ph_2PCH_2PPh_2)]$ **3d**

Atom	*x*	*y*	*z*	Atom	*x*	*y*	*z*
Os(1)	0.8467(1)	0.7998(1)	0.2223(1)	C(32)	0.5120(29)	0.8837(21)	0.2639(18)
Os(2)	0.7236(1)	0.8911(1)	0.1240(1)	O(32)	0.4293(20)	0.9014(19)	0.2639(17)
Os(3)	0.6526(1)	0.8522(1)	0.2693(1)	C(33)	0.6949(25)	0.9419(20)	0.3217(19)
P(1)	0.9741(6)	0.8991(4)	0.2356(4)	O(33)	0.7285(25)	0.9951(17)	0.3503(17)
P(2)	0.8383(6)	1.0002(4)	0.1308(4)	C(101)	1.0914(14)	0.8972(10)	0.1772(12)
C(1)	0.7035(20)	0.7462(15)	0.2048(14)	C(102)	1.1099	0.8388	0.1235
C(2)	0.6428(21)	0.7924(15)	0.1602(14)	C(103)	1.1996	0.8410	0.0791
C(3)	0.6774(30)	0.6612(24)	0.2340(22)	C(104)	1.2707	0.9015	0.0884
C(4)	0.5393(27)	0.7662(20)	0.1212(20)	C(105)	1.2521	0.9599	0.1421
C(5)	0.9207(19)	0.9968(14)	0.2161(14)	C(106)	1.1625	0.9578	0.1865
F(1)	0.7334(22)	0.6416(12)	0.2916(15)	C(111)	1.0289(18)	0.9105(11)	0.3312(11)
F(2)	0.7031(25)	0.6121(10)	0.1775(14)	C(112)	1.0940	0.8506	0.3560
F(3)	0.5828(21)	0.6476(15)	0.2449(22)	C(113)	1.1317	0.8509	0.4305
F(4)	0.5596(18)	0.7105(13)	0.0697(16)	C(114)	1.1045	0.9111	0.4802
F(5)	0.4712(18)	0.7356(18)	0.1669(13)	C(115)	1.0395	0.9710	0.4554
F(6)	0.4949(16)	0.8214(12)	0.0808(12)	C(116)	1.0017	0.9707	0.3809
C(11)	0.9316(24)	0.7150(18)	0.2057(17)	C(201)	0.9369(15)	1.0190(9)	0.0578(10)
O(11)	0.9810(23)	0.6612(14)	0.1852(17)	C(202)	0.9493	0.9682	−0.0037
C(12)	0.8551(27)	0.7766(19)	0.3333(19)	C(203)	1.0258	0.9826	−0.0581
O(12)	0.8695(33)	0.7652(20)	0.3928(14)	C(204)	1.0898	1.0478	−0.0511
C(13)	0.8449(20)	0.8089(13)	0.0942(13)	C(205)	1.0774	1.0986	0.0104
O(13)	0.8845(17)	0.7804(13)	0.0474(10)	C(206)	1.0009	1.0842	0.0648
C(21)	0.6166(28)	0.9570(22)	0.1330(21)	C(211)	0.7704(16)	1.0940(12)	0.1373(9)
O(21)	0.5444(18)	1.0030(13)	0.1403(17)	C(212)	0.7679	1.1396	0.2032
C(22)	0.6979(21)	0.8846(18)	0.0175(16)	C(213)	0.7103	1.2084	0.2046
O(22)	0.6792(20)	0.8769(15)	−0.0453(11)	C(214)	0.6552	1.2318	0.1401
C(31)	0.6303(36)	0.8013(27)	0.3599(26)	C(215)	0.6577	1.1863	0.0742
O(31)	0.6171(25)	0.7656(19)	0.4186(18)	C(216)	0.7153	1.1174	0.0728

Tables 4 and 5. The structures confirm the μ_3-$\eta^2(\|)$ coordination mode of the alkyne ligands. The overall geometry of the two structures is similar, and the high estimated standard deviations preclude a detailed comparison of the structural parameters between the two clusters. The Os atoms in each case define an isosceles triangle the longest edge of which is bridged both by a carbonyl and by the $Ph_2PCH_2PPh_2$ ligand. All the Os–Os lengths are significantly shorter than the average distance of 2.877(3) Å in the parent carbonyl, $[Os_3(CO)_{12}]$.[20] However, the distances are similar to the values found in $[Os_3(CO)_{10}(PhC_2Ph)]$,[21] where the alkyne also adopts the μ-$\eta^2(\|)$ bonding mode. The bridging alkyne presumably exerts a metal–metal bond-shortening influence compared to the unbridged case. The ligand distribution differs significantly between $[Os_3(CO)_{10}(PhC_2Ph)]$ and complexes **3c** and **3d**. In $[Os_3(CO)_{10}(PhC_2Ph)]$ there is an asymmetric ligand distribution with two incipient bridging carbonyls lying close to the Os_3 plane; this reflects the electron imbalance within the cluster.[21] In both **3c** and **3d** there is a much more symmetric ligand distribution, and the single bridging carbonyl is close to symmetric. The presence of the chelating phosphine ligand, which is a better σ donor than two carbonyl ligands, may be responsible for this structural difference.

Despite the large difference in electronic properties of CF_3

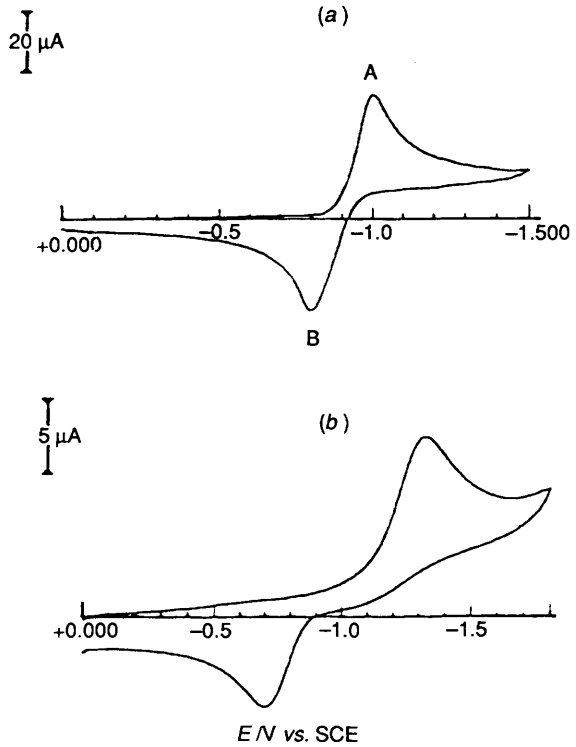

Fig. 5 Cyclic voltammograms recorded on a CH_2Cl_2 solution containing compound **2a** (7.5×10^{-4} mol dm^{-3}) and $[NBu_4][ClO_4]$ (0.2 mol dm^{-3}). Scan rate 0.2 V s^{-1}, T = 20 °C. Electrodes: (*a*) mercury, (*b*) platinum

and Me substituents, the alkynes $CF_3C{\equiv}CCF_3$ and $MeC{\equiv}CMe$ have thus been shown to give μ_3-η^2(∥) co-ordination modes, whereas $PhC{\equiv}CPh$ and *p*-$MeC_6H_4C{\equiv}C_6H_4Me$-*p* give predominantly μ_3-η^2(⊥) co-ordination. Furthermore, attempts to decarbonylate $[Os_3(CO)_8(RC_2R)(Ph_2PCH_2PPh_2)]$ (R = Me **3c** or CF_3 **3d**) both thermally (in refluxing toluene) or using Me_3NO did not give any evidence for the formation of $[Os_3(CO)_7\{\mu_3$-η^2(⊥)-$RC_2R\}(Ph_2PCH_2PPh_2)]$ complexes. It thus seems reasonable to propose that the ⊥ co-ordination mode arises due to steric effects.

Electrochemical Investigations.—Fig. 5 shows the cyclic voltammetric response exhibited by $[Os_3(CO)_7(PhC_2Ph)(Ph_2PCH_2PPh_2)]$ **2a** in dichloromethane solution, both at a platinum and a mercury electrode. A single reduction process is displayed, peaks A and B, which was shown by controlled-potential coulometry at both a mercury pool (E_w = −1.2 V) and a platinum gauze (E_w = −1.5 V) to consume two electrons per molecule. Concomitantly, the solution turns from a wine red to a golden-yellow colour. The resulting solution is EPR silent. Cyclic voltammetry on this exhaustively reduced solution gives responses fully complementary with those reported in Fig. 5, so indicating the full chemical reversibility of this two-electron addition.

The changes in the IR spectrum during the two-electron reduction have been recorded by means of an optically transparent thin-layer electrochemical (OTTLE) cell. The initial spectrum consists of the following ν_{CO} bands: 2052m, 1980s, 1960 (sh) and 1920w cm^{-1} (Table 1). After exhaustive reduction the spectrum shows the following bands: 1952m, 1890s, 1871s, 1829m and 1798w cm^{-1}. There are several isosbestic points and no evidence of any monoanion intermediate.

It is clearly evident from the shapes of the voltammograms illustrated in Fig. 5 that the electrode material affects the rate of the reduction process. The mercury electrode, not unusually,[22,23] favours the heterogeneous electron transfer. The diagnostic parameter for this kinetic behaviour is the peak-to-peak separation, which is 198 mV at the mercury electrode and 626 mV at the platinum electrode, at the representative scan rate of 0.2 V s^{-1}. The sluggishness of the electron transfer is somewhat related to the reorganisational barrier accompanying the **2a**–**2a**$^{2-}$ redox change.[24] An electrochemically reversible two-electron transfer which does not involve a significant structural rearrangement is expected to display a ΔE_p value of 29 mV, which should remain constant with changing scan rate.[25] In fact, even at the more favourable mercury electrode, we observed a progressive increase of ΔE_p from 122 mV at 0.02 V s^{-1} to 374 mV at 2.0 V s^{-1}. These features are also observed in acetone solution. This means that, independently of the electrode material and solvent, a structurally significant reorganisation accompanies the conversion of the 46-electron $[Os_3(CO)_7(PhC_2Ph)(Ph_2PCH_2PPh_2)]$ **2a** into the 48-electron $[Os_3(CO)_7(PhC_2Ph)(Ph_2PCH_2PPh_2)]^{2-}$. We confidently assign such a structural change to the ⊥–∥ alkyne reorientation discussed above.

A plot of E *vs.* $\log[(i_d - i)/i]$ from polarographic analysis in acetone solution was linear with a slope of 38 mV. This value, higher than the 29.5 mV expected for a Nernstian two-electron step, further supports the quasi-reversibility of the **2a**–**2a**$^{2-}$ reduction.

In order to compute the standard heterogeneous electron-transfer rate, k_s(app), we measured, by chronocoulometry at the mercury electrode, the diffusion coefficient D of compound **2a** in acetone solution. The value was found to be 6.2×10^{-6} cm^2 s^{-1}. The use of the extended working curve ΔE_p *vs.* Ψ (where Ψ is a dimensionless parameter related to ΔE_p)[26] allowed us to compute a k_s value of $(2.2 \pm 0.5) \times 10^{-4}$ cm s^{-1}, which approaches that found for the two-electron transfer $[Os_6(CO)_{18}] \longrightarrow [Os_6(CO)_{18}]^{2-}$, namely $(4.5 \pm 0.7) \times 10^{-4}$ cm s^{-1}.[26] Interestingly, the rearrangement of the bicapped-tetrahedral $[Os_6(CO)_{18}]$ to the closed-octahedral $[Os_6(CO)_{18}]^{2-}$ involves breaking and reforming Os–Os bonds, whereas the rearrangement of the *closo*-trigonal-bipyramidal **2a** to the *nido*-octahedral **2a**$^{2-}$ requires the breaking and reforming of Os–C bonds.

Further confirmation of the ⊥–∥ alkyne reorientation was obtained by a study of the redox chemistry of $[Os_3(CO)_7(p$-$MeC_6H_4C_2C_6H_4Me$-$p)(Ph_2PCH_2PPh_2)]$ **2b**, which proved to be useful in the ^{1}H NMR investigation described above. As expected, the electrochemical behaviour of **2b** parallelled that of **2a**. The infrared spectrum of the dianion **2b**$^{2-}$, obtained by macroelectrolysis in acetone solution containing $LiClO_4$ (0.1 mol dm^{-3}) as supporting electrolyte, was quite similar to that of **2a**$^{2-}$, testifying to a similar structure. After removal of the solvent, **2b**$^{2-}$ was dissolved in CD_2Cl_2 (in which $LiClO_4$ is almost insoluble) and sealed in an NMR tube. The proton NMR spectrum indicates that **2b**$^{2-}$ is diamagnetic; in addition, the two methyl groups of the tolyl ligands are equivalent (singlet at δ 2.42), thus indicating a symmetrical co-ordination of the alkyne (*i.e.* parallel), as previously illustrated for $[Os_3(CO)_8(p$-$MeC_6H_4C_2C_6H_4Me$-$p)(Ph_2PCH_2PPh_2)]$ **3b**.

In contrast to the propensity of the present 46-electron clusters **2a** and **2b** to add reversibly two electrons (Table 6), all the 48-electron complexes **3a**–**3d** exhibit a single-step two-electron reduction process, chemically irreversible in character, at very negative potential values, in accordance with the fact that the lowest unoccupied molecular orbital (LUMO) of these closed-shell compounds lies at a higher energy level and possesses metal–metal antibonding character.

The cyclic voltammetric responses shown in Fig. 6 are very informative. These compare the redox behaviour of the 46-electron cluster **2a** with that of the related 48-electron cluster **3a**, obtained by bubbling CO through a deaerated acetone solution of **2a**. It is clear that the thermodynamically unstable 50-electron species $[Os_3(CO)_8(PhC_2Ph)(Ph_2PCH_2PPh_2)]^{2-}$, instantaneously generated at the peak C, converts quickly,

through a decarbonylation reaction, into the 48-electron cluster $[Os_3(CO)_7(PhC_2Ph)(Ph_2PCH_2PPh_2)]^{2-}$, which, as discussed above, reversibly loses two electrons to give $[Os_3(CO)_7(PhC_2Ph)(Ph_2PCH_2PPh_2)]$ **2a** at the peak system B/A.

Finally, the stable dianion $[Os_3(CO)_7(PhC_2Ph)(Ph_2PCH_2PPh_2)]^{2-}$ produced by exhaustive electrolysis can be protonated at 0 °C by CF_3CO_2H to give the neutral species $[Os_3H_2(CO)_7(PhC_2Ph)(Ph_2PCH_2PPh_2)]$ **4**. Interestingly the isoelectronic dianion $[Fe_3(CO)_9(EtC_2Et)]^{2-}$ reacts with CF_3CO_2H (under the same experimental conditions) to reform the parent compound $[Fe_3(CO)_9(EtC_2Et)]$, with H_2 evolution. This different behaviour can be traced back to the lower thermodynamic stability of Fe–H compared to Os–H bonds.[27] We have also synthesised the dihydrido-cluster **4** by direct hydrogenation of **2a**. Thus electrochemical reduction (two-electron) followed by protonation ($2H^+$) represents a *redox-mediated* hydrogenation reaction (Fig. 7).

The ^1H and ^{31}P NMR spectra of compound **4** clearly indicate that the two hydride ligands bridge non-equivalent edges of the Os_3 triangle. The spectroscopic data do not enable us to determine the mode of co-ordination of the alkyne. However, the electrochemical behaviour of **4**, which is very similar to that of **3a–3d**, suggests **4** has a similar structure.

Experimental

All reactions were carried out under nitrogen using dried, degassed solvents. Infrared spectra were recorded on a Perkin Elmer 681 spectrophotometer using CH_2Cl_2 solutions, mass spectra on a VG707E instrument, and NMR spectra in $CDCl_3$ using a JEOL EX400 spectrometer. The compound $[Os_3(\mu\text{-H})(CO)_8\{\mu\text{-}Ph_2PCH_2P(Ph)C_6H_4\}]$ **1** was prepared as previously described.[28]

Preparation of $[Os_3(CO)_7(PhC_2Ph)(Ph_2PCH_2PPh_2)]$ **2a**.—Diphenylacetylene (0.20 g, 0.10 mmol) was added to a toluene solution (40 cm^3) of $[Os_3H(CO)_8\{Ph_2PCH_2P(Ph)C_6H_4\}]$ (0.08 g, 0.07 mmol) with stirring at 80 °C. After 5 h the red solution was evaporated to dryness and purified by TLC. Elution with CH_2Cl_2–heptane (1:1) gave a major red band (0.05 g, 50%) of compound **2a** (Found: C, 41.3; H, 2.6%; *M*, 1329. $C_{46}H_{32}O_7Os_3P_2$ requires C, 41.5; H, 2.4%; *M*, 1329).

Reaction of Compound **2a** *with* CO.—Carbon monoxide was bubbled through a solution of compound **2a** (0.059 g, 0.04 mmol) in toluene (25 cm^3) at room temperature for 0.5 h. The resulting orange solution was evaporated to dryness to give an analytically pure sample of $[Os_3(CO)_8(PhC_2Ph)(Ph_2PCH_2PPh_2]$ **3a** (Found: C, 41.2; H, 2.6%; *M*, 1357. $C_{47}H_{32}O_8Os_3P_2$ requires C, 41.6; H, 2.4%; *M*, 1357).

Preparation of $[Os_3(CO)_7(p\text{-}MeC_6H_4C_2C_6H_4Me\text{-}p)(Ph_2PCH_2PPh_2)]$ **2b**.—This compound was prepared in the same

Table 6 Redox potentials (in V *vs.* SCE) for the electrochemical processes undergone by clusters **2–4**

Complex	$E(0 \longrightarrow 2-)$/ V	n^a (±0.2)	$(i_p^a/i_p^c)^b$	Solvent
2a	−0.80[c]	2	1	Me_2CO
	−0.90[c]	2	1	$CHCl_3$
2b	−0.78[d]	2	1	Me_2CO
3a	−1.40[d]	2	0	Me_2CO
3b	−1.42[d]	2	0	Me_2CO
3c	−1.53[d]	2	0	Me_2CO
3d	−1.18[d]	2	0	Me_2CO
4	−1.93[d]	2	0	Me_2CO

[a] Determined by coulometry at a mercury pool. [b] At room temperature and at 0.2 V s^{-1} scan rate. [c] Formal electrode potential $E = (E_p^a + E_p^c)/2$ for chemically reversible processes. [d] Peak potential value, E_p, referred to 0.2 V s^{-1} scan rate.

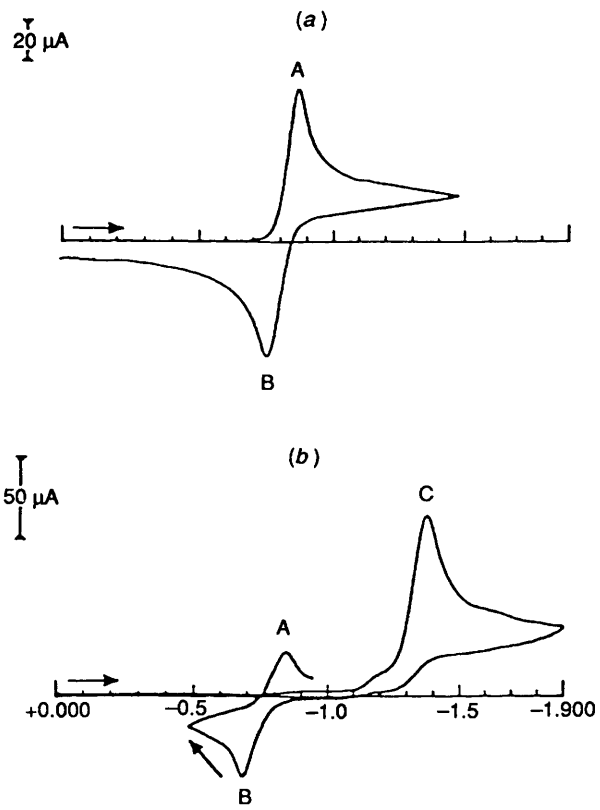

Fig. 6 Cyclic voltammograms recorded at a mercury electrode on an acetone solution containing compound **3a** (1.8×10^{-3} mol dm^{-3}) and $[NBu_4][ClO_4]$ (0.2 mol dm^{-3}). Scan rate 0.2 V s^{-1}; T = 20 °C. (*a*) Initial; (*b*) after bubbling CO through the solution for 15 min

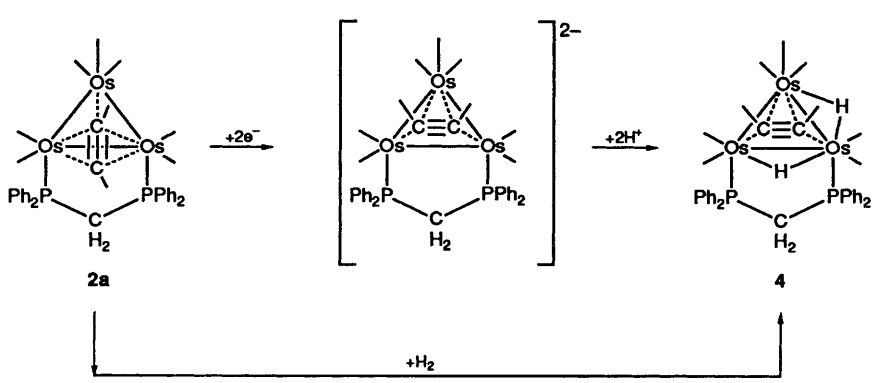

Fig. 7 The transformation of compound **2a** into **4**

way as for **2a** but using *p*-$MeC_6H_4C{\equiv}CC_6H_4Me$-*p* as ligand to give **2b** as a red solid in 20% yield (Found: C, 42.6; H, 2.6%; *M*, 1357. $C_{48}H_{36}O_7Os_3P_2$ requires C, 42.5; H, 2.7%; *M*, 1357).

Preparation of $[Os_3(CO)_8(MeC_2Me)(Ph_2PCH_2PPh_2)]$ **3c**.—But-2-yne (1.0 g, 8.5 mmol) was added to a toluene solution (30 cm^3) of $[Os_3H(CO)_8\{Ph_2PCH_2P(Ph)C_6H_4\}]$ (0.10 g, 0.084 mmol) in a flask fitted with a CO_2–acetone condenser. The solution was heated to 80 °C with stirring for 8 h. The resulting solution was evaporated to dryness and purified by TLC to give compound **3c** as an orange solid (0.06 g, 60%) (Found: C, 35.8; H, 2.2%; *M*, 1233. $C_{37}H_{28}O_8Os_3P_2$ requires C, 36.0; H, 2.3%; *M*, 1233).

Preparation of $[Os_3(CO)_8(CF_3C_2CF_3)(Ph_2PCH_2PPh_2)]$ **3d**.—A toluene solution (30 cm^3) of $[Os_3H(CO)_8\{Ph_2PCH_2P(Ph)C_6H_4\}]$ (0.10 g, 0.084 mmol) was sealed under 100 Torr (*ca.* 1.33×10^4 Pa) of hexafluorobut-2-yne in an ampoule (200 cm^3). The ampoule was placed in a thermostatic tank at 80 °C for 2 d. The resulting orange solution was evaporated to dryness and purified by TLC to give compound **3d** (0.05 g, 50%) (Found: C, 33.2; H, 1.9%; *M*, 1341. $C_{37}H_{22}F_6O_8Os_3P_2$ requires C, 33.1; H, 1.7%; *M*, 1341).

Reaction of Compound **2a** *with* H_2.—Hydrogen was bubbled through a solution of compound **2a** (0.059 g, 0.04 mmol) in toluene (30 cm^3) at reflux temperature for 2 h. The resulting dark yellow solution was filtered through a small silica column (in order to eliminate the metallic residue) and then evaporated to dryness. Crystallisation from CH_2Cl_2–hexane (10:90 v/v) gave an analytically pure yellow sample of $[Os_3H_2(CO)_7(PhC_2Ph)(Ph_2PCH_2PPh_2)]$ **4** (90%) (Found: C, 41.9; H, 2.4%; *M*, 1331. $C_{46}H_{34}O_7Os_3P_2$ requires C, 41.5; H, 2.6%; *M*, 1331).

Electrochemical Studies.—Voltammetric measurements were performed with two sets of instrumentation: a PAR 273 or a BAS 100A analyser connected to an interfaced IBM microcomputer. A standard three-electrode cell was designed to allow the tip of the reference electrode (saturated calomel, SCE) closely to approach the working electrode. Positive feedback *iR* compensation was applied routinely. All measurements were carried out under N_2 in anhydrous deoxygenated solvents. The temperature of the solution was kept constant within 1 °C, by circulation of a thermostatted water–ethanol mixture through the double wall of the cell. The working electrode was a platinum disk electrode (area *ca.* 0.8 mm^2) embedded in a Teflon seal or a similar gold disk electrode amalgamated by dipping in mercury.

Potential data (V *vs.* SCE) were checked against the ferrocene (0–1+) couple added as an internal standard. Under the actual experimental conditions the ferrocene–ferrocenium couple is located at +0.46 V in CH_2Cl_2 and +0.48 V in acetone.[29] The number of electrons transferred (*n*) in a particular redox process was determined by controlled-potential coulometry at a platinum basket or at a mercury pool; all experiments were done in duplicate.

X-Ray Structure Determination of $[Os_3(CO)_8(MeC_2Me)(Ph_2PCH_2PPh_2)]$ **3c**.—Crystals of complex **3c** were grown from an acetone–ethanol solution and a suitable orange crystal of dimensions 0.3 × 0.3 × 0.3 mm was selected.

Crystal data. $C_{37}H_{28}O_8Os_3P_2$, $M = 1233$, orthorhombic, space group $P2_12_12_1$, $a = 12.6072(12)$, $b = 17.0015(37)$, $c = 17.3419(29)$ Å, $U = 3717.1$ Å^3 (by least-squares refinement of angles from 25 reflections), Mo-Kα radiation, $\lambda = 0.710\,69$ Å, $D_m = 2.21$ g cm^{-3}, $Z = 4$, $D_c = 2.20$ g cm^{-3}, $F(000) = 2287$, $\mu = 104.38$ cm^{-1}.

Data collection and processing. Nonius CAD-4 diffractometer (Queen Mary College, London), ω–2θ scan mode, 3673 unique reflections recorded ($\theta_{max} = 25°$, *h* 0–15, *k* 0–20, *l* 0–20) of which 3661 with $F_o > 6\sigma(F_o)$ were used in refinement. Empirical absorption correction based on azimuthal scans applied. Three standard reflections showed no significant intensity variation during data collection.

Structure Analysis and Refinement.—The osmium atoms were located by heavy-atom methods and the remaining non-hydrogen atoms by Fourier techniques (SHELX 76[30]). Least-squares refinement was carried out keeping all atoms isotropic. A semiempirical absorption correction (DIFABS[31]) was then applied to the data. Further least-squares refinement (anisotropic Os, P and O atoms) was carried out. The phenyl rings were constrained to be regular hexagons (C–C 1.395 Å, C–C–C 120°) with individual isotropic vibration parameters assigned to each carbon atom. All hydrogen atoms were placed in calculated positions (C–H 1.08 Å) and refined isotropically. The weighting scheme, $w = 62.4242/[\sigma^2(F) + 0.000\,007F^2]$, gave satisfactory agreement analyses. Final *R* and *R'* values were 0.058 and 0.06. Atom scattering factors were taken from ref. 32. A list of fractional atomic coordinates is given in Table 4.

X-Ray Structure Determination of $[Os_3(CO)_8(CF_3C_2CF_3)(Ph_2PCH_2PPh_2)]$ **3d**.—Crystals of complex **3d** were grown from hexane–CH_2Cl_2 (70:30).

Crystal data. $C_{37}H_{22}F_6O_8Os_3P_2$, $M = 1341.09$, orthorhombic, space group $P2_12_12_1$ (no. 19), $a = 12.906(9)$, $b = 17.130(7)$, $c = 17.547(10)$ Å, $U = 3879(2)$ Å^3, $Z = 4$, $D_c = 2.30$ g cm^{-3}, λ(Mo-Kα) = 0.710 69 Å, $\mu = 99.6$ cm^{-1}, $F(000) = 2480$, $T = 17$ °C.

Data collection and reduction. A dark red plate with dimensions (distances to faces from centre) 0.067(110, $1\bar{1}0$) × 0.210($1\bar{1}0$, $\bar{1}10$) × 0.133($\bar{1}01$, $10\bar{1}$) × 0.152($10\bar{1}$, $\bar{1}01$) mm was mounted on a glass fibre with epoxy resin and transferred to a Stoe four-circle diffractometer. A total of 5820 reflections were measured (ω–2θ scan mode) in the range $5 \leqslant 2\theta \leqslant 45°$, of which 4877 were unique (R_{int} 0.045) and 3956 considered observed [$F > 6\sigma(F)$]. A numerical absorption correction was applied, with transmission factors 0.04–0.34. Cell constants were refined from diffractometer angles of 50 reflections in the 2θ range 20–25°.

Structure solution and refinement. The structure was solved by an automated Patterson method (to locate the Os atoms) and subsequent Fourier difference techniques. It was refined by blocked full-matrix least squares with Os, P, F and O assigned anisotropic thermal parameters. The phenyl rings were refined as regular hexagons (C–C 1.395 Å), and phenyl and methylene hydrogens were placed in idealised positions and allowed to ride on the relevant carbon (C–H 1.08 Å); phenyl and methylene hydrogens were assigned common isotropic thermal parameters. The weighting scheme was $w^{-1} = \sigma^2(F) + 0.007F^2$. Refinement on *F* led to converged residuals of $R = 0.065$, $R' = 0.071$. A final Fourier difference map showed no significant electron density except for ripples close to the Os atom positions (*ca.* 3 e Å^{-3}). The structure was solved using SHELX 86[33] and refined with SHELX 76.[30] Final atomic coordinates are given in Table 5.

Additional material available from the Cambridge Crystallographic Data Centre comprises H-atom coordinates, thermal parameters and remaining bond lengths and angles.

Acknowledgements

We thank the SERC for studentships (to P. A. D. and A. J. M.), Professor M. B. Hursthouse for the X-ray data collection of **3c** (SERC Crystallography Service), and Johnson Matthey for a generous loan of OsO_4. We are indebted to Professor Geiger (University of Vermont) for the plot of ΔE_p *vs.* Ψ and for helpful discussions. M. A. thanks the European Economic Community for a mobility grant under the ERASMUS scheme.

References

1 E. Sappa, A. Tiripicchio and P. Braunstein, *Chem. Rev.*, 1983, **83**, 203; D. Osella and P. R. Raithby, in *Stereochemistry of Organometallic and Inorganic Compounds*, ed. I. Bernal, Elsevier, Amsterdam, 1988, vol. 3.
2 J. F. Blount, L. F. Dahl, C. Hoogzand and W. Hübel, *J. Am. Chem. Soc.*, 1966, **88**, 292.
3 V. Busetti, G. Granozzi, S. Aime, R. Gobetto and D. Osella, *Organometallics*, 1985, **3**, 1510.
4 A. D. Clauss, J. R. Shapley and S. R. Wilson, *J. Am. Chem. Soc.*, 1981, **103**, 7387.
5 M. Tachikawa, J. R. Shapley and C. G. Pierpont, *J. Am. Chem. Soc.*, 1975, **97**, 7172.
6 S. Rivomanera, G. Lavigne, N. Lugan and J. J. Bonnet, *Organometallics*, 1991, **10**, 2285.
7 S. Aime, R. Gobetto, L. Milone, D. Osella, L. Violano, A. J. Arce and Y. De Sanctis, *Organometallics*, 1991, **10**, 2854.
8 A. J. Arce, Y. De Sanctis and A. J. Deeming, *Polyhedron*, 1988, **7**, 979.
9 M. I. Bruce, P. A. Humphrey, H. Miyamae and A. H. White, *J. Organomet. Chem.*, 1991, **417**, 431.
10 A. J. Deeming, S. Hasso and M. Underhill, *J. Chem. Soc., Dalton Trans.*, 1975, 1614.
11 A. J. P. Domingos, B. F. G. Johnson and J. Lewis, *J. Organomet. Chem.*, 1972, **36**, C43.
12 D. Boccardo, M. Botta, R. Gobetto, D. Osella, A. Tiripicchio and M. T. Camellini, *J. Chem. Soc., Dalton Trans.*, 1988, 1249 and refs. therein.
13 B. E. R. Schilling and R. Hoffmann, *J. Am. Chem. Soc.*, 1979, **101**, 3456; *Acta Chem. Scand., Ser. A*, 1979, **33**, 231.
14 G. Granozzi, E. Tondello, M. Casarin, S. Aime and D. Osella, *Organometallics*, 1983, **2**, 430.
15 S. Aime, R. Bertoncello, V. Busetti, R. Gobetto, G. Granozzi and D. Osella, *Inorg. Chem.*, 1986, **25**, 4004.
16 D. Osella, R. Gobetto, P. Montangero, P. Zanello and A. Cinquantini, *Organometallics*, 1986, **5**, 1247.
17 R. S. Dickson and O. M. Paravegne, *Organometallics*, 1991, **10**, 721.
18 J. A. Clucas, P. A. Dolby, M. M. Harding and A. K. Smith, *J. Chem. Soc., Chem. Commun.*, 1987, 1829.
19 S. Rivomanera, G. Lavigne, N. Lugan and J. J. Bonnet, *Inorg. Chem.*, 1991, **30**, 4112.
20 M. R. Churchill and B. C. DeBoer, *Inorg. Chem.*, 1978, **16**, 87.
21 C. G. Pierpont, *Inorg. Chem.*, 1977, **16**, 636.
22 S. W. Blanch, A. M. Bond and R. Colton, *Inorg. Chem.*, 1981, **20**, 755.
23 W. J. Bowyer and W. E. Geiger, *J. Electroanal. Chem. Interfacial Electrochem.*, 1988, **239**, 253 and refs. therein.
24 A. Cinquantini, G. Opromolla and P. Zanello, *J. Chem. Soc., Dalton Trans.*, 1991, 3161 and refs. therein.
25 E. R. Brown and J. R. Sandifer, in *Physical Methods of Chemistry. Electrochemical Methods*, eds. B. W. Rossiter and J. F. Hamilton, Wiley, New York, 1986, vol. 2, ch. 4.
26 B. Tulyathan and W. E. Geiger, *J. Am. Chem. Soc.*, 1985, **107**, 5960.
27 R. G. Pearson, *Chem. Rev.*, 1985, **85**, 41.
28 J. A. Clucas, D. F. Foster, M. M. Harding and A. K. Smith, *J. Chem. Soc., Chem. Commun.*, 1984, 949.
29 W. E. Geiger, in *Organometallic Radical Processes*, ed. W. C. Trogler, Elsevier, Amsterdam, 1990, p. 144.
30 G. M. Sheldrick, SHELX program for Crystal Structure Determination, University Chemical Laboratory, Cambridge, 1976.
31 N. Walker and D. Stuart, *Acta Crystallogr., Sect. A*, 1983, **39**, 158.
32 *International Tables for X-Ray Crystallography*, Kynoch Press, Birmingham, 1974, vol. 4.
33 G. M. Sheldrick, SHELX 86 program for solution of crystal structures, University of Göttingen, Göttingen, 1986.

Received 29*th September* 1992; *Paper* 2/05245H